

## Applications of Fractal Dimension

Edrees, M. N. Mahmood \*

### ABSTRACT

Today the method of determining the dimension is being applied to many kinds of observations, especially to time series in physics, engineering, and in fields as far apart as meteorology and neurophysiology. This paper has selectively surveyed some recent work in the vast and rapidly growing area on the behavior of the fractal dimension. We used the concept of dimension to distinguish between random noise and chaos, also to determine the order of Non-Linear Auto-regressive Model, finally it used to test the residuals of linear models

### تطبيقات البعد الشذوي

#### الملخص

تعد طريقة تحديد البعد في الآونة الأخيرة من المجالات التي شهدت تطبيقاً واسعاً وعلى مختلف أنواع التجارب، خاصةً على السلاسل الزمنية الفيزيائية، الهندسية، وفي حقول علم الأنواء الجوية والفيزياء النووية. أن الهدف من هذا البحث هو أعداد مسح لبعض التطورات الحديثة على سلوك البعد الشذوي. إذ تم استخدام مفهوم البعد في هذا البحث للتمييز بين النظم الفوضوية والنظم العشوائية وكذلك لتحديد رتبة نموذج الانحدار الذاتي غير الخطي واخيراً تم استخدامه لاختبار بواقي النماذج الخطية.

\*College of Computers Sciences and Mathematics/University of Mosul.

Received: 4/ 1 /2006

Accepted: 23/ 2 / 2006

## 1. Introduction

Many natural phenomena are better described using a fractional dimension, and fractals are thus used as descriptive models for the growth of plants, particle aggregation, river cartography, realistic images, and similar phenomena. Their fractal dimension characterizes most of these fractal models. In physical systems, the fractal dimension reflects some properties of the system. The physical characteristics of some bodies are related to the fractal dimension of their surfaces. For example, the growth pattern of bacteria has a fractal dimension of 1.7, and the fractal dimension of clouds is 1.30 to 1.33; for snowflakes it is 1.7, for coastlines in South Africa or Britain, 1.05 to 1.25, and for woody plants and trees, 1.28 to 1.90. In medicine, fractal dimension have been found for various biomolecules such as DNA and proteins. For instance, the fractal dimension of lysozyme (egg-white) is 1.614; for hemoglobin it is 1.583, and for myoglobin 1.728. The fractal dimension of the perimeter of surface cell sections has been used to distinguish healthy cells from cancerous cells. In analytical chemistry, the fractal dimension is used as a tool to characterize chemical patterns and problems of sample homogeneity. A given fractal dimension makes it possible to simulate a variety of systems: fluid extraction or contaminant mitigation techniques, the hybrid orbital model of proteins, or the growth of conflict rate in aircraft flight schedules. In the last years, fractal geometry has provided a new approach to traditional methods of antenna design. Several classical fractals of the initiator-iterator kind (for example, Von Koch's snowflake, Sierpinski's gasket) have been proposed as antenna prototypes. Certain properties of fractal antennae are related to their fractal dimension: An increase in the fractal dimension may be translated into higher gain, low return loss, and a shifting down of the resonant frequencies (Ortega et al., 2003). Fractal dimension provides an objective meaning for comparing fractals and they can be attached to clouds, trees, coastlines, feathers, networks of neurons in the body, dust in the air at an instant in time, the clothes we are wearing, the

distribution of frequencies of the light reflected by a flower, the colors emitted by the sun, and the wrinkled surface of the sea during a storm (Barnsley, 1993).

## 2. Basic Concepts

A fractal dimension of a set is a number that tells us how densely the set occupies the metric space in which it lies. It is invariant under various stretching and squeezing of the underlying space. This makes the fractal dimension meaningful as an experimental observable, it possesses a certain robustness and independent of the measurement units.

The starting point is an attempt to generalize notions of geometric “size” of sets lying in  $R^n$ , from the conventional ideas of “length” ( $n=1$ ), “area” and “arc length” ( $n=2$ ), and “volume” and “surface area” ( $n>2$ ), in cases in which the complexity of the sets of interest prohibits meaningful categorization by these familiar measures. The most readily understood class of measures involves the notion of trying to “cover” the set of interest, say  $S$ , lying in a compact subset of  $R^n$ , with  $n$ -dimensional boxes with sides of length  $\epsilon$ , small number. If  $n=1$  and  $S$  is simply an interval of length  $L$ , clearly the “number” of “boxes” used to cover the interval is approximately, ignoring integer part corrections,  $N(S, \epsilon) = L / \epsilon$ . For  $S$ , a  $n$ -dimension cube with side  $L$ , we have  $N(S, \epsilon) = (L / \epsilon)^n$ . For such nice sets  $S$ , a little algebra suggests the usual interpretation of the dimension of  $S$  :

$$n = \lim_{\epsilon \rightarrow 0} \frac{\log N(S, \epsilon)}{\log(1 / \epsilon)} .$$

Different measures of dimension are based on this notion of “covering”  $S$ . For example, for an arbitrary, compact set  $S$  lying entirely in  $R^n$  to be covered by  $n$ -dimensional cubes, define the capacity of  $S$  (or the fractal dimension of  $S$ ) as (for more details see Gulick, 1992):

$$d_c = \lim_{\epsilon \rightarrow 0} \frac{\log N(S, \epsilon)}{\log(1 / \epsilon)} .$$

Capacity dimension is the simplest and is useful for illustrating what a fractional dimension means. It, however, treats the attractor as a static geometrical object ignoring the fact that there is a dynamical flow defined on it (and defining it). In a simulation or experiment, the attractor is not seen directly, only typical trajectories over finite time periods are observed. Thus capacity is of questionable use in a practical setting and serves as an upper bound to the fractal dimension of an attractor (see e.g. Parker and Chua, 1987).

There are other measures of dimension in addition to this mentioned above. Some of the measures often studied in the chaos literature may be motivated by the suggestion that one relate the geometry of attractors, the structure of ergodic distribution and the mathematical properties of chaos. For practical purposes the correlation dimension is strictly related to the fractal dimension (Berliner, 1992). To briefly discuss this, let us start with the 1-dimensional series,  $\{\mathbf{x}_t\}_{t=1}^k$ , and from this form the sequence of  $N = k - m + 1$   $m$ -dimensional vectors

$$\mathbf{X}_s = \{\mathbf{x}_s, \mathbf{x}_{s+1}, \dots, \mathbf{x}_{s+m-1}\}_{s=1}^{k-m+1}$$

The obtained plot is called phase portrait. In the dynamical systems literature, the ambient space in which we do the viewing is called the embedding space, its dimension  $m$  is called the embedding dimension and each  $\mathbf{X}_s$  is known as an  $m$ -history of the series  $\{\mathbf{x}_t\}_{t=1}^k$ . This converts the original scalar series into a shorter series of  $N$  ( $m$ -dimensional) vectors with overlapping entries. Assuming that the true, but unknown, system which generated  $\{\mathbf{x}_t\}_{t=1}^k$  is  $\theta$ -dimensional and provided that  $\mathbf{m} \geq 2\theta + 1$ , then the set of  $m$ -history recreates the dynamics of the data generation process and can be used to analyze the dynamics of the system. This is the basic content of the celebrated Takens theorem, (see Takens, 1981), which extends the classic embedding theorem of Whitney in topology to dynamical systems. The correlation dimension is obtained by considering the correlation integral, defined by Grassberger and Procaccia, (1983) as

$$C(N, m, \epsilon) = \frac{2}{N(N-1)} \#\{(s, t) : 1 \leq s, t \leq N\},$$

where # denotes the number of elements in the set. The correlation integral is related to the correlation dimension by the power law  $C(\epsilon) \sim \epsilon^D$  ( $\epsilon \rightarrow 0$ ). This results in the correlation dimension  $D_c^m$  being defined as

$$D_c^m = \lim_{\epsilon \rightarrow 0} \frac{\log(C(N, m, \epsilon))}{\log(\epsilon)}$$

for  $m=1, 2, 3, \dots, j$  for  $j$  no larger than around 10.

The correlation dimension is a probabilistic type of dimension and is theoretically provides a lower bound to the fractal dimension of an attractor.

We now give some basic applications of the fractal dimension

### 1. Generation Fractal Objects

We can set up some iterative procedures to generate fractal objects using a given value for the fractal dimension. With other procedures, we may be able to determine the fractal dimension from the properties of the constructed object. The fractal dimension  $d_c$  of an object is always greater than the corresponding Euclidean dimension (or topological dimension), which is simply the least number of parameter, needed to specify the object. An Euclidean curve is one-dimensional, an Euclidean solid is three-dimensional. For a fractal curve that lies completely within a two-dimensional plane, the fractal dimension  $d_c$  is greater than 1 (the Euclidean dimension of a curve). The closer  $d_c$  is to 1, the smoother the fractal curve. If  $d_c = 2$ , we have a peano curve, that is, the “ curve “ completely fills a finite region of two-dimension space. For  $2 < d_c < 3$ , the curve self-intersects and the area could be covered an infinite number of times. Fractal curve can be used to model natural object boundaries, such as shorelines. Spatial fractal curve (those that do not lie completely within a single plane) also have fractal dimension  $d_c$  greater than 1, but  $d_c$  can be greater than 2 without self-intersecting. A curve that fills a volume of space has dimension  $d_c = 3$ , and a self-

intersecting space curve has a fractal dimension  $d_c > 3$ . Fractal surfaces typically have a dimension within the range  $2 < d_c < 3$ . If  $d_c = 3$ , the “ surface “ fills a volume of space. And if  $d_c > 3$ , there is an overlapping covering of the volume. Terrain, clouds, and water are typically modeled with fractal surfaces. The dimension of a fractal solid is usually in the range  $3 < d_c < 4$ . Again, if  $d_c > 4$ , we have a self-overlapping object. Fractal solid can be used, for example, to model cloud properties such as water-vapor density or temperature within a region of space (Hearn and Baker, 1997). By adjusting the fractal dimension we can obtain highly realistic representation for terrain and other natural objects using affine fractal methods that model object features as fractional Brownian motion. This is an extension of standard Brownian motion, a form of “ random walk “, that describes the erratic, zigzag movement of particles in a gas or other fluid. Figure (1) illustrates a random-walk path in the xy plane.

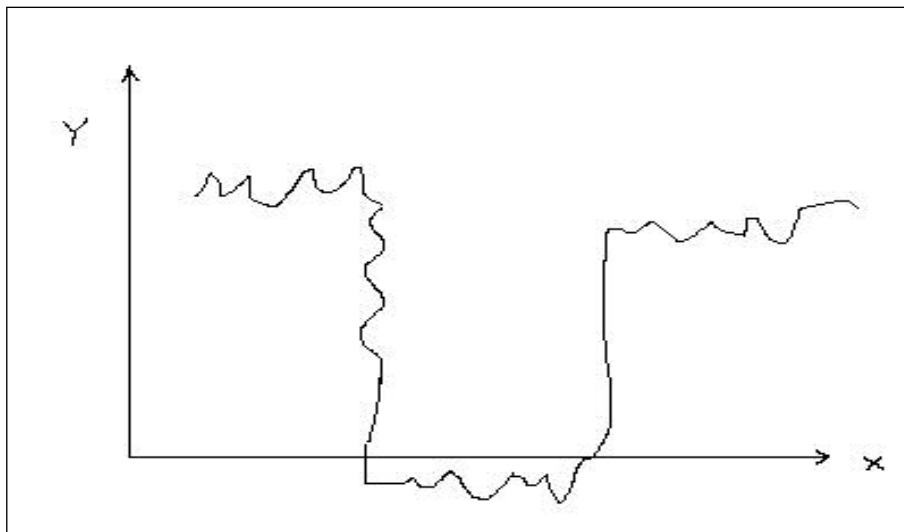


**Figure (1). An example of Brownian motion (random walk) in the xy plane.**

Starting from a given position, we generate a straight-line segment in a random direction and with a random length. We then move to the end point of the first line segment and repeat the process. This procedure is repeated for any number of line

segments, and we can calculate the statistical properties of the line path over any time interval  $t$ . Fractional Brownian motion is obtained by adding an additional parameter to the statistical distribution describing Brownian motion. This additional parameter sets the fractal dimension for the (motion) path, for more details see (Barnsley et al., 1988).

Another method of generating statistically self-similar point sets (fractal sets) is called Levy flight. In a Levy flight, one “flies” from one point to the next by a length  $\Delta x$  that is distributed according to a homogeneous (and thus scale-invariant) power law,

$$Pr ob (\Delta x > \varepsilon) \sim \varepsilon^{-d_c} .$$

For a one-dimensional Levy flight and  $d_c = 0.5$ , one finds the distribution of the  $0_s$  of the gambler’s ruin. For a tree-dimensional flight (with directions isotropically selected over the solid angle) and  $d_c = 1.23$  one obtains the astronomically observed “lumpy” distribution of galaxies in our universe (Schroeder, 1989).

### 3. Classification of Attractors

In this section, we classify attractors using the concept of dimension. An attractor could be defined to be  $n$ -dimensional if, in a neighborhood of every point, it looks like an open subset of  $R^n$ . This is how the dimension of a manifold is defined in different topology. For instance, a limit cycle is one-dimensional since it looks locally like an interval. A torus is two-dimensional since, locally, it resembles an open subset of  $R^2$ . An equilibrium point is considered to have zero dimensions. The neighborhood of any point of a strange-attractor, however, has a fine structure and does not resemble any Euclidean space. Hence, strange attractors are not manifolds and do not have integer dimension, see table 1 (Parker and Chua, 1987).

**Table (1). Classification of Attracting sets.**

<b>Steady State</b>	<b>Flow</b>	<b>Dimension</b>
Periodic	Closed Curve	1
Equilibrium Point	Point	0
Two-Periodic	Tours	2
K-Periodic	K-Tours	K
Chaotic		Non integer

## 2. Randomness and Chaos

There is a deep philosophical question concerning the difference between determinism and stochasticity or (randomness). Indeed it can be said that the more you think about randomness the less random things get. Define (random process) to be a process whose dimension is (high). A (deterministic process) is a process with (low) dimension (Brock and Sayers, 1998). Chaos theory deals with deterministic processes which look random but whose dimension is finite. Here, we are concentrating on low dimensional chaos and how to distinguish it from a random process. One of the characteristic measures of a chaos is its fractal dimension, which allows one to distinguish between deterministic chaos and randomness (Yamazaki and Mino, 1989). Grassberger and Procaccia (1983) suggested the correlation dimension as a tool for distinguishing random from chaotic time series. If, as embedding dimension increases,  $D_C^m$  continues to rise then this is symptomatic of a stochastic system. If, however, the data are generated by a deterministic process (consistent with chaotic behavior), then  $D_C^m$  will reach a finite limit at some relatively small  $m$ . The correlation dimension can therefore be used to distinguish true stochastic processes from deterministic chaos (which may be low-dimensional or high-dimensional). Figure (2) illustrates the theoretical relationship between  $\log(C(N, m, \epsilon))$  and  $\log(\epsilon)$  (see Chappell and Eldridge,



1997). For  $a \leq \log(\epsilon) \leq b$ ,  $\epsilon$  is too small and very few  $m$ -histories lie with a distance  $\epsilon$  of each other. For  $\log(\epsilon) > c$ ,  $\epsilon$  is too large and all  $m$ -histories will lie within a distance  $\epsilon$  of each other. For  $b < \log(\epsilon) < c$ ,  $C(N, m, \epsilon)$  increases as  $m$  increases;  $C(N, m, \epsilon)$  is the slope of the line for  $b < \log(\epsilon) < c$ . This slope will increase initially as  $m$  is increased.

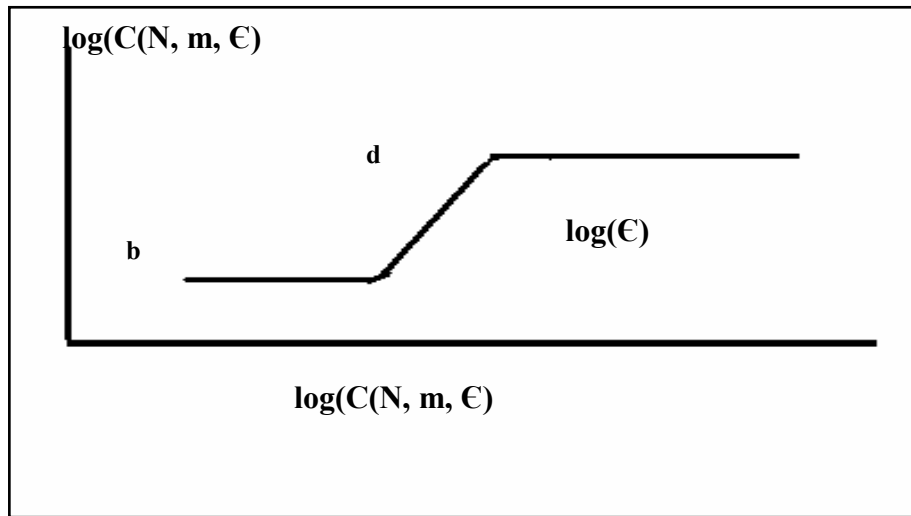


Figure (2). Theoretical relationship between  $\log(C(N, m, \epsilon))$  and  $\log(\epsilon)$ .

As mentioned above, if the data under consideration contain a detectable non-linear deterministic component, the correlation dimension should increase with increasing values of the embedding dimension. However, this should level off at some point and remain constant for all further values of the embedding dimension. On the other hand, if the true data generating process is purely random, then we would expect the correlation dimension always to increase with the embedding dimension.

**Application:** To show how powerful is the dimensional method to distinguish between deterministic chaos and randomness. The method is verified on two synthetic time series of 3000 data points. The first synthetic time series is a realization of Henon Map, given by

$$x_{t+1} = 1 + y_t - a x_t^2$$

$$y_{t+1} = b x_t, \text{ with } a=1.4 \text{ and } b = 0.3.$$

Unlike the previous signal, the second consists of purely random series (Gaussian white noise).

For each of the two sampled time series, we use the Grassberger and Procaccia method to compute the correlation dimension, and the results are shown in figure (3).

As can be seen from figure (3), the dimensional estimates of the Henon attractor (chaotic) converge to a finite value with  $D_C^m = 1.2 \pm 0.01$ . Contrast this case with the case when the time series is purely random the correlation dimension keeps on increasing as a function of the embedding dimension and there is no sign that this levels off at some point. Thus it would seem that the correlation dimension would tend to measure the dimension of the noise as opposed to the underlying dynamics which are of interest.

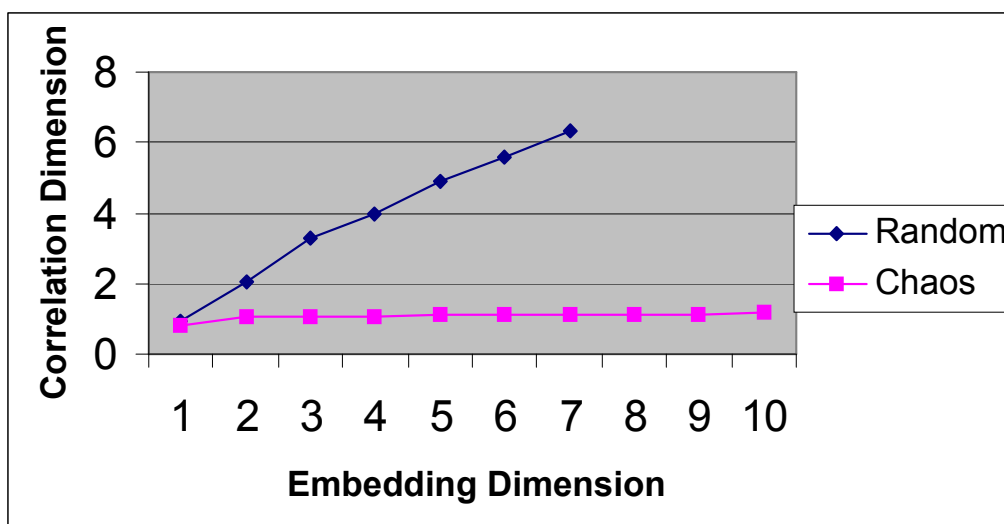


Figure 3. Relationship between  $D_C^m$  and  $m$  for a chaotic series and a purely random series.

#### 4. Order of Non-Linear Auto-regressive Model

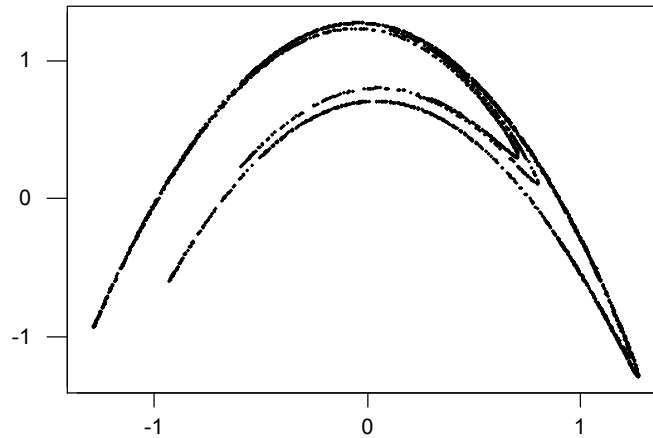
Estimation of dimension might give indications of the number of lags that one should fit in non-linear auto-regressions if linear auto-regressions do not fit well (Brock and Sayers, 1998).

The basic idea is a quite simple : to view a 1- dimensional object, say a loop, unambiguously we only need to live in a space not bigger than a 3-dimensional space. ( Needless to say, going beyond 3 will enable us to view the same object equally unambiguously but 3 will be sufficient to guarantee unambiguity.) If the loop is non-intersecting, then we need to go all the way to 3. In other cases, a lower dimension will often suffice. More generally, to view an attractor say  $A$  unambiguously, we need to live in an  $m$ -dimensional space. In short,  $1 + 2 \dim(A)$  is the smallest dimension which will guarantee unambiguous viewing for all attractors of dimension  $\dim(A)$ , however "weird". Just as going beyond the embedding dimension will not yield any additional information about the geometric structure of the attractor  $A$ , going beyond the order of a non-linear auto-regressive model will add nothing to the probabilistic structure of the stochastic process. Thus, the two concepts are linked at least at this level (Tong, 1994).

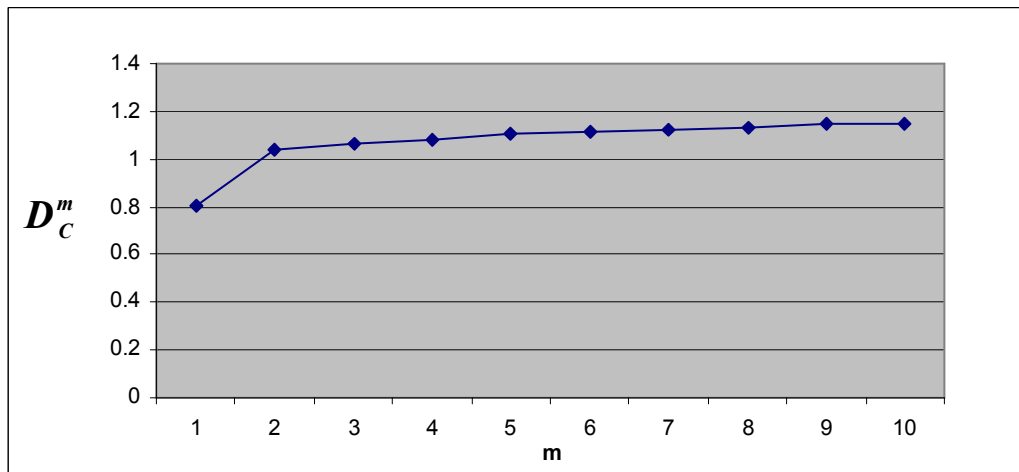
For an embedding to be suitable for successful estimation of dimension, one must choose suitable values of embedding dimension. Recently, there have been many discussions on how to determine the appropriate embedding dimension for a scalar time series. one is that the correlation theorem is employed to estimate appropriate embedding dimension ( see e.g. Takens, 1981; Grassberger and Procaccia, 1983).

That is, by increasing the embedding dimension, one notes, an appropriate dimension  $m$  when the value of the correlation dimension stops changing. Thus, the dimension estimates is computed for increasing embedding dimension  $m$  until the dimensional estimate stabilizes. This final  $D_c^m$  is the proper value of the correlation dimension, and the lowest  $m$  yielding this value is the minimal dimension of the reconstruction space.

Figure(4) shows a phase portrait obtained by applying Takens procedure to the Henon time series. The correlation dimension  $D_c^m$  obtained in this way is shown in figure(5) as a function of the embedding dimension  $m$  for the Henon time series. With increasing  $m$ ,  $D_c^m$  increases and becomes nearly constant,  $D_c^m = 1.2 \pm 0.01$ , and the lowest  $m$  yielding this value is 2 and we need at least two equations to construct the time series.



Figure(4). The Henon attractor.



Figure(5). Correlation dimension  $D_C^m$  in Henon as a function of m

## 5. Whiteness Diagnostic

Estimates of dimension can be machined into methods to test the adequacy of linear models of both trend stationary and difference stationary type (Brock and Sayers, 1998). We can perform the whiteness diagnostic using the  $\log(C(N, m, \epsilon))$  versus  $\log(\epsilon)$  plot.

The whiteness diagnostic compared the dimensional estimates obtained from the correlation dimension for the residuals with dimensional estimates for a series of Gaussian pseudo random numbers of the same length, mean, and variance. If the two series have the same  $D_C^m$ , then this is consistent with the residuals under scrutiny being Gaussian white noise. Evidence of non whiteness of the residuals which shows different estimates of  $D_C^m$  for the two series. i.e. the difference between the original and the putatively white residuals sample correlation estimates should be statistically significant.

**Application:** We demonstrate the application of the above method with computational simulation of a linear system

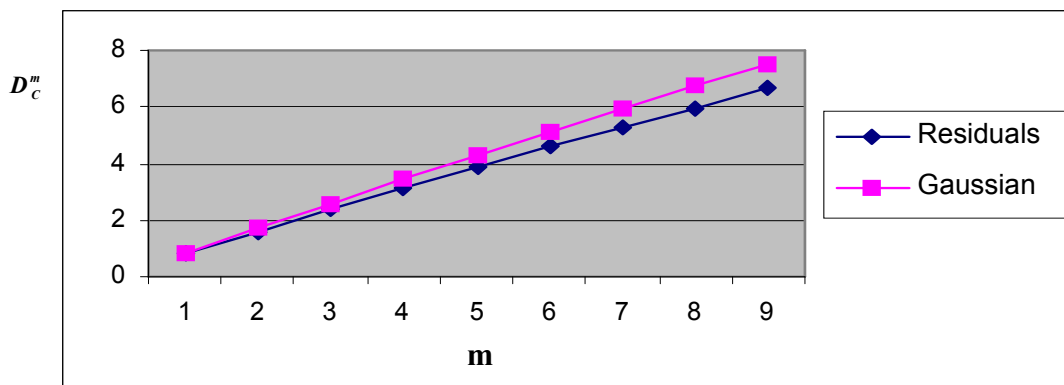
$Y_t = 0.8X_{t-5} - 0.6X_{t-6} + 0.4X_{t-7} + e_t$ , where  $e_t$  is the model error. Two samples of the Y component are considered of this

system. Let us consider two models to show how powerful is the method to examine the performance and importance of the choice of modeling algorithm, the first model is  $Y_t = 0.00061 + 0.719X_t + e_t$ , and the second (after logarithmic transformation to the data points) is  $Y_t = -0.0854 + 0.906X_t + e_t$ . A regression analysis of the two models is shown in Table(2).

**Table(2). Regression Analysis**

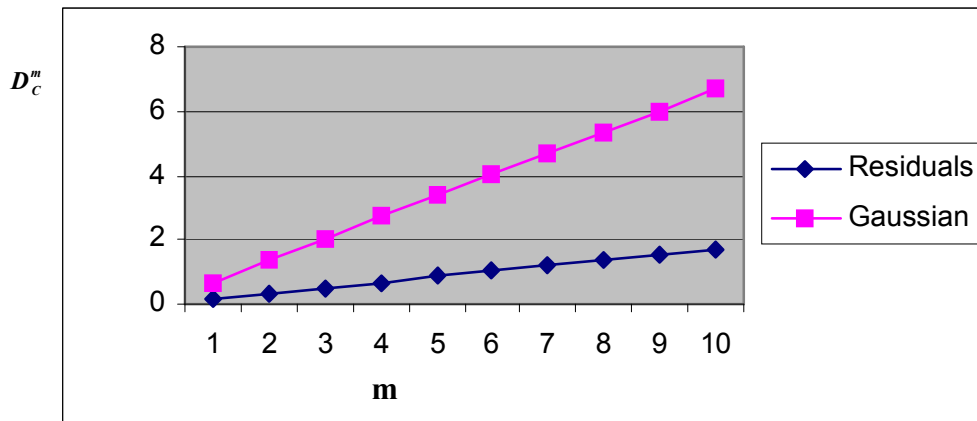
Model (1)						
Source	DF	SS	MS	F	R-sq.	R-sq.(adj.)
Regression	1	36698	36698	412247.79	99.6 %	99.6 %
Residual Error	1491	133	0			
Total	1492	36830				
Model (2)						
Source	DF	SS	MS	F	R-sq.	R-sq.(adj.)
Regression	1	293.04	293.04	8828.81	85.6 %	85.5 %
Residual Error	1491	49.49	0.03			
Total	1492	342.53				

We have constructed our own Gaussian Pseudo random numbers and compared it with residuals of model (1) to test the accuracy of it. We found that the two estimates are similar (as it should) according to the correlation dimension (see figure 6).



**Figure(6). Dimensional estimate of model (1).**

The same procedure has been applied to model (2). An analysis of the correlation integral yields clear evidence of non whiteness of the residuals. As is seen in figure 7, the dimensional estimates for the two series are different.



Figure(7). Dimensional estimate of model (2).

## 6. Spectral Indices

In a lot of practically important cases, the power spectral density has a power-law, i.e., low frequencies have higher energies compared to high frequencies following the unique relationship

$$p(f) \propto f^{-\beta} .$$

Here  $p(f)$  is the power spectral density,  $f$  is the frequency, and  $\beta$  is a power-law index. A curve with a single power-law index for all frequencies is self-similar (Koszma et al., 1998). The following approximate relationship has been obtained (Higuchi, 1990) between power-law index  $\beta$  and the fractal dimension  $d_c$ : over the range of  $1 \leq d_c \leq 2$ ,

$$d_c = E + (3 - \beta) / 2$$

for a function of Euclidean dimension  $E$ .

Note that the above relation is just an approximation. It holds for a class of processes called fractional Brownian motion with  $1 < \beta < 3$ , but it breaks down for  $\beta < 1$  and  $\beta > 3$  for more details see (Kozma et al., 1998).

## 7. Hurst Exponent

In 1951 Hurst found long-term correlation in fluctuation of outflows from the Nile River. He discovered that hydrological time series show longer periods of droughts and floods than were to be expected if the processes had both finite memory and variance (Van de Giesen and Mata, 2002). His work was based on the methods used for reservoir design. The design of a reservoir seeks to determine the optimum capacity that will allow ideal performance over a range of years. The capacity that allows the reservoir to produce a uniform outflow and never empty or overrun is determined by adjusting a rivers cumulative discharge for the year by the sample average for the set of years in question,  $n$ . The difference between the maximum and minimum of these adjusted value is denoted by  $R(d)$ , and is the optimum capacity for the reservoir.

Using  $R(\Delta t)$ , otherwise known as the range, as a tool to investigate actual behaviour of river discharge records Hurst found that the cumulative fluctuations in outflow satisfied the following power law

(Hastings and Kissell, 1998) :

$$\text{range}\{y(s) : t \leq s \leq t + n\} = \text{const} \times n^H.$$

Where the range is defined as the maximum deviation of cumulative actual behaviour from average behaviour within a sample. Mandelbrot and Wallis later confirmed that it was valid to model geophysical records using fractional noises (Mandelbrot and Wallis, 1969).

The Hurst exponent,  $H$ , is a self-similarity parameter that measures the long-range dependence in a time series, and provides a measure of long-term non-linearity. The expected value of  $H$  lies between 0 and 1. For  $H=0.5$  the cumulative behavior is a random walk and the process produces uncorrelated white noise. However in the cases where the Hurst exponent is either greater than or less than 0.5 there are underlying non-linear dynamics in the system.  $H < 0.5$  represents anti-persistent behavior and  $H > 0.5$  is fractional Brownian motion with increasing persistence strength as  $H$  approaches 1 (Lange, 2003).



The process for estimating the Hurst exponent can be found in both (Weron, 2002) and (Peters, 1994). Hurst exponent estimation has been applied in areas ranging from biophysics to computer networking. However, the modern techniques for estimating the Hurst exponent comes from fractal mathematics (Ian, 2003). For a relationship between the power-law exponent  $\beta$ , the Hurst exponent, and the fractal dimension  $d_c$  is given (Barnsley et al., 1988) by  $\beta=2H+1=5-2d_c$ . The Hurst exponent,  $H$ , and the fractal dimension,  $d_c$ , are related by the equation  $H = E + 1 - d_c$ , where  $E$  is the Euclidean dimension (  $E = 0$  for a point, 1 for a line, 2 for a surface ). For one-dimensional signals,  $H = 2 - d_c$ .

**Example ( Hurst exponent of Henon )**

Using the equation outlined above the estimated value of the Hurst exponent for the Henon time series with  $a=1.4$  and  $b=0.3$  is approximately 0.7. The value of  $H$  is greater than 0.5 indicating that the time series is not random i.e. there is memory in the data and persistent behaviour.

**8. Auto-correlation functions**

The mathematical definition of long-memory processes is given in terms of auto-correlation. When a data set exhibits auto-correlation, a value  $X_i$  at time  $t_i$  is correlated with a value  $X_{i+s}$  at time  $t_{i+s}$ , where  $s$  is some time increment in the future. In a long memory-process auto-correlation decays over time and the decay follows a power law. A time series constructed from 30-day returns of stock prices tends to show this behavior. In a long-memory process the decay of the auto-correlation function for a time series is a power law:

$$P(k) = C k^{-\alpha}$$

where  $C$  is a constant and  $P(k)$  is the auto-correlation function with lag  $k$ . The Hurst exponent is related to the exponent alpha in the equation by (Ian, 2003 ):

$$H = 1 - \frac{\alpha}{2} .$$

The value of the Hurst exponent ranges between 0 and 1.

Since the power spectrum is the Fourier transform of the auto-correlation function, one can find the following relationship between the auto-correlation exponent  $\alpha$  and the power spectrum exponent  $\beta$ :  $\alpha = 1 - \beta$ , where  $0 < \alpha < 1$ . The exponent  $\alpha$  is related to the fractal dimension  $d_c$  by the equation :  $\alpha = 2 d_c - 2E$

## 9. Conclusions

There are various numbers, associated with fractals, which can be used to compare them. They are generally referred to as fractal dimension. Fractal dimension is important because it can be defined in connection with real-world data, and it can be measured approximately by means of experiments.

Based on the examples in this paper, the fractal dimension technique appears to be a viable method for :

- 廈 Distinguishing between randomness and chaos.
- 廈 Indicating the order of nonlinear auto-regressive model.
- 廈 Testing the adequacy of the model.
- 廈 Estimating the Hurst exponent.

## References

- Barnsley, M. F, Devaney, R. L, Mandelbrot, B. B, Peitgen, H. D, Saupe, D, and Voss, R. F. (1988). "The Science of Fractal Images". Springer-Verlag, New York.
- Barnsley, M. F. (1993) "Fractals Everywhere". Second Edition, Academic Press Inc, New York.
- Beran, J. (1994). "Statistics for Long-memory Processes", Chapman and Hall, New York.
- Berliner, L. M. (1992). "statistics, probability and chaos." Statistical Science, Vol. 7, No.1, PP 69-90.
- Brock, W. A. and Sayers, C. L, (1998)." Is the business cycle characterized by deterministic chaos ?." Forthcoming in Journal of Economics.
- Chappell, D., and Eldridge, R.M. (1997). " Nonlinear characteristics of the Sterling/ECU exchange rate: 1984-1992, The European Journal of Finance, 3, PP 159-182.
- Grassberger, P., and Procaccia, (1983). " Measuring the Strangeness of Strange Attractors", Physica 9D, PP 189-208.
- Gulick, D. (1992). " Encounters With Chaos. " McGraw-Hill, Inc.
- Hastings, H. M. and Kissells, R. (1998)." Is the Nile Outflow Fractal? Hurst's Analysis Revisited". Natural Resource Modeling, Vol. 11, No. 2, PP 83- 93.
- Hearn, D. and Baker, M. P. (1997). " Computer Graphics C Version." Prentice-Hall International Inc.
- Higuchi, T. (1990). "Relationship between the fractal dimension and the power law index for a time series : A numerical investigation", Physica D, 46, 254 .
- Hurst, H. E. (1951). " Long-Term Storage Capacity of Reservoirs". Transactions of the American Society of Civil Engineers. 116, PP 770-808.
- Ian Kaplan ,(2003). " Estimating the Hurst Exponent. htm".
- Kozma, R., Kasabov, N. K , and Kim, J .S .(1998) . "Integration of Connectionist Methods and Chaotic Time-Series Analysis for the Prediction of Process Data", International Journal of intelligent systems, Vol. 13, PP 519-538.

- Lange, H. (2003). " Time Series Analysis of Ecosystem Variables with Complexity Measures". [http://www. bitoeck. uni-bayreuth. de/~ Holder. Lange /iccs2/lange.htm](http://www.bitoeck.uni-bayreuth.de/~Holder.Lange/iccs2/lange.htm). Visited, March 11th, 2003.
- Mandelbrot, B. B. and Wallis, J. R. ( 1969). " Some Long-Run Properties of Geophysical Records". *Water Resources Research*, Vol. 5, NO. 2, PP 321-340.
- Ortega, A., Dalhoum, A. A., and Alfonseca, M. (2003). " Grammatical evolution to design fractal curves with a given dimension ". *IBM J. RES. & DEV.* Vol. 47 No. 4 PP 483-492.
- Park, K. and Willinger, W. (2000). " Self-similar network traffic: an overview, in: *Self-similar Network Traffic and Performance Evaluation*", edited by Park, K. and Willinger, W. New York, NY: Wiley, 2000, PP 1-38.
- Parker, T. S. and Chua, L. D. (1987). " Chaos tutorial for engineers". *Proceeding of the IEEE*, Vol. 75, No. 8, PP 982-1008.
- Peters, E. E. ( 1994). " Fractal Market Analysis : Applying Chaos Theory to Investment and Economics", John Wiley and Sons Inc.
- Schroeder, M. R. (1989). "Self-similarity and fractals in science and art " *.J. Audio Eng. Soc.* Vol. 37, No. 10, PP 395-808.
- Takens, F. (1981). " Detecting strange attractors in turbulence ". *Dynamical Systems and Turbulence. Lecture Notes in Math.* 898 PP 366-381. Springer, New York.
- Takens, F. (1985). " On the numerical determination of the dimension of an attractor ". *Dynamical Systems and Bifurcations. Lecture Notes in Math.* 1125 PP 99-106. Springer, New York.
- Tong, H. (1994). " A personal overview of nonlinear time series analysis from a chaos perspective ". Invited lecture at the 15th Nodic Conference on Mathematical Statistics Lund, Sweden, 1994.
- Van de Giesen, N and Mata, L. J. (2002). " Comparison of the Hurst exponents of Historical and GCM rainfall time series". *Hydrology Days*.
- Weron, R. (2002). " Estimating long-range dependence : finite sample properties and confidence intervals", *Physica A.* 312, PP 285-299.
- Yamazaki, H and Mino, M. (1989). " Chaos in spin-wave instabilities ". *Theoretical Physica. Supplemen*, No. 98.